MecSol2013
International Symposium on Solid Mechanics
April 18-19, 2013
Porto Alegre, Rio Grande do Sul, Brazil

Computational Analysis Considering Ageing Effects on a Wind Turbine Blade

Julio Cesar Pinheiro Pires
PGDesign
Federal University of Rio Grande do Sul
arquitoca@gmail.com

Clarissa Coussirat Angrizani
PPGEM
Federal University of Rio Grande do Sul
cangrizani@hotmail.com

Branca Freitas de Oliveira
PGDesign
Federal University of Rio Grande do Sul
branca@ufrgs.br

Sandro Campos Amico
PPGEM
Federal University of Rio Grande do Sul
amico@ufrgs.br

ABSTRACT

Nowadays polymeric composites are being used as alternative materials in structural applications, such as civil, automotive and energy industry. These materials suffer degradation of the polymeric matrix caused by different environmental factors. In this work, studies of accelerated ageing in hot water were conducted for estimating ageing effects on a polymer fiber-glass composite. The composite specimens were molded, aged and then tested. After determining the mechanical properties of the specimens, the results were transferred to the computer simulation by finite element analysis in software Abaqus. A small wind turbine blade of 1m length is simulated. The study of durability and managing the end of service life of these devices become important as an increasing number of wind turbines are installed worldwide. Operating conditions were applied according to predetermined loads considering thrust and rotational force due to the wind action. Computer simulations considering failure analysis were conducted in order to optimize the used composite layer to maintaining a cost-effective design, in addition to understanding the life cycle of the material. The methods proposed in this work intend to provide forecasts for durability studies of products using polymeric composites structures.

Keywords: Composite Materials, Ageing, Wind Turbine, Finite Element Analysis

1 INTRODUCTION

The search for renewable energy sources is of global concern because of issue of shortage of raw material, pollution and waste. Thus, despite the high cost of deploying and necessity to

favorable environmental conditions, if used long time, the use of solar and wind energy can be an alternative.

Wind turbines have three basic components, the rotor blades, the gondola (nacelle) and the tower. In gondola are located the main components, electrical generator, box responsible for speed, shafts and bearings among others. This work will be focused on blades.

The blades are elements that come into direct contact with the air flow. The moment of interaction of the blades with the wind is when kinetic energy is transferred from the surface of the blade.

Nowadays the most common material used for manufacturing blades for horizontal axis wind turbines is the composite reinforced with glass fibers. The blade made of glass fiber was layered to obtain good mechanical properties and low density (compared aluminium) since one of the requirements is to get more power each day [1].

Several variables are present when determining a geometry which requires controlled behavior during the contact with the fluid. According to [2], to obtain an efficient design of the blades, some goals must be met:

- maximize energy production for a specific distribution of wind;
- seek the maximum power limit;
- resist loads inherent to the object and the fatigue that can occur;
- restrict tendency of movement of the tip of the blade toward the tower;
- avoid resonances;
- minimize weight and cost.

The aerodynamic loads are decisive for the lifetime of wind turbines. According to [3], prior to the design of a new blade, it takes into account its structural design to ensure that the blade supports all loads.

The wind turbine blades are designed and constructed to resist forward with a range of 20 to 30 years in operation [3]. Cracks in specific locations due to the cycles of use can significantly reduce the lifetime of this material. According to [4], currently the blades are made of composite materials because they can satisfy complex design, have low weight and good stiffness properties.

The composites are usually used as layer to form plates, shells or other two-dimensional elements. Thus it is possible to manufacture composite parts, for example, using different layers with different fibre directions. These directions are defined according to design requirements such as dimensions of parts (thickness), tension direction, shear force direction and according to the use of the part. [5]. The possibility of designing the material according to specific needs makes composites widely employed in industry for wind turbines.

On the other hand there is the problem of disposal of the composites, because currently the mechanical recycling of thermoset matrices composites is reduced; and chemical and energy recycling are not economically viable in Brazil [6]. The matrix has a great influence on composite material properties, because it determines the resistance of the composite to most degradative processes that eventually cause failure of the structure, including impact, damage, delamination, water absorption, chemical attack, corrosion and oxidation resistance. [7]

In this study hot water aging is used to obtain aged material properties. In future works other accelerated aging environments will be analysed. Hygrothermal aging has been studied in articles like [8] that analyses the tensile properties of glass fibre/epoxy composite made by hand lay-up process. After degradation test in hot water (80 °C / 0, 3, 10, 100h, 300h) no stabilization in water absorption was observed and modulus and strength had a declining trend. Other authors such as [9] [10] [11] [12] [13] [14] studied the behaviour of the material/product in environments of accelerated degradation, in order to optimize the design of new products.

In this work glass fibre/epoxy unidirectional composites with %Vf of 37% were produced and shear and tensile properties were obtained for simulating a wind turbine blade using Abaqus CAE 6.10-1(Dassault Systèmes 2010) to compare non-ageing and ageing situations.

The design described in this paper takes into account the low manufacturing cost, high performance and simplicity. According to [15], the manufacturing cost of the blades of a wind turbine is around 15 to 20% of the total production cost of the turbine. This justifies the conduct of scientific research in order to reduce equipment costs, adding security, and maximize efficiency in energy conversion.

The methodology followed to achieve the objectives of this research is presented as follows:

a. identification and status of the issue in the energy context;
b. conducting exploratory research literature review on wind turbines and accelerated ageing studies;
c. performing geometric modelling in three-dimension (3D), applying concepts of aerodynamic profiles for wind turbine blades, considering the maximum power that can be converted from the wind;
d. determination of the aerodynamic forces acting on blades of wind turbines;
e. performing hot water ageing for composite material
f. determination of the composite properties for ageing and non-ageing situations
g. performing structural analysis simulation of the blade using finite element method;
h. applying a composite failure criterion in the simulation;
i. comparison of results for three lamination types.

2 GEOMETRY OF THE BLADE

The design of the rotor blades must take into account structural and aerodynamic aspects. Within the scope streamlined, it can be listed some stages of the project:

- definition of the diameter of the rotor;
- definition of the geometry of the airfoil;
- definition of the aerodynamic parameters (pitch angle, speed);
- definition of the geometry of the longitudinal profile of the blade (longitudinal twisting);

a) Diameter of the rotor

The rotor is formed by the parties that allow the rotation of the shaft and transmit spin to the generator. The blades are the main elements that form the rotor. The diameter of the rotor is directly related to the performance of the turbine. This relationship is presented in Eq. 1

$$P_{dis} = \frac{1}{2}\rho A v^3 \qquad (1)$$

Where the wind power available, P_{dis}, is directly proportional to air density, ρ, the area swept by the rotation of the blades, A, and the cube of wind speed, v.

Thus, the length of the blades is defined by the power wanted to be removed from the wind and converted into electricity.

b) Geometry of the airfoil

There are several airfoils designed for use in wind turbines. However most of these projects are originated from the wings of aircraft.

This research defined the lift coefficient *Cl* as the main measure of efficiency of the profile to be chosen. The drag coefficient, *Cd*, was also considered in the analysis, as in the case of a small rotor the goal is to "find" a satisfactory ratio between lift and drag to control the speed, resulting from angular velocity and wind speed.

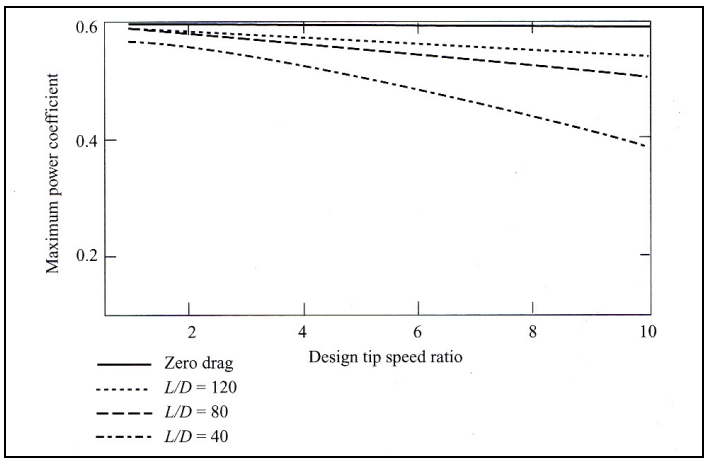

Figure 1: Lift (L) and drag (D) on the coefficient of power and speed specific
Source: [1]

As shown in Fig. 1 the more increases the specific speed (tip speed ratio), more is needed to have a design that leverages the lift (*L*).

The profile analysis was conducted with the aid of the software *JavaFoil*, available on the website of Professor Dr. Martin Hepperle, University of Stuttgart, Germany [16]. This software was developed in *Java* language and has its main use in the analysis of wing profiles for aircraft models. Some concepts of aerodynamics applied to airfoils of aircraft wings can be applied to analysis of blades for wind turbines.

The profile initially chosen was the MH110, also developed by Martin Hepperle. This airfoil is drawn from the coordinate points in two dimensions (x and y axes).

After entering the coordinates, it is possible to visualize the shape of the airfoil (Fig. 2).

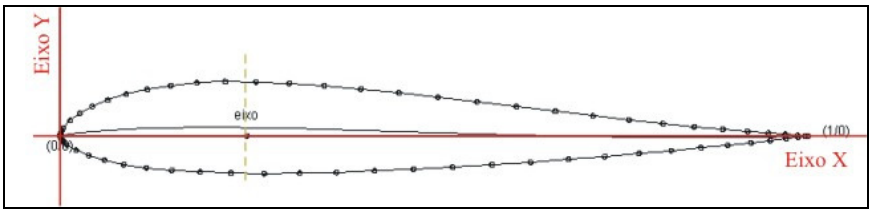

Figure 2: Form the airfoil MH110

This profile was created from 68 points in Cartesian coordinates. The maximum thickness (t/c) of the profile is 11.959% at 26.2% of the x-axis. The curvature (f/c), which is the mid-surface between the top and bottom edge of the profile has the maximum value of 1.088% at 22.7% of the x-axis.

With the airfoil created, it is possible to determine which angle of the profile will have more lift, drag and pressure (in this case, wind power). To analyze wing aircraft, the angle of attack is directly linked to the variables listed above, as the aircraft wing is interacting only with one wind direction, i.e., the calculation is done by shifting the wing and not by the displacement of fluid (wind).

In the case of the wind rotor, there are two components to consider: the wind and the rotation of the blades. From a speed that is the result of a geometric sum of these two speeds it can be determined the angle of attack. Thus the angle of attack of blades for wind turbines is not constant as in airplane wings. But the pitch angle is fixed. Therefore it is clear the importance of the adequacy of the design of the blades to arrive at an angle of attack such that a greater lift is achieved.

c) Aerodynamic parameters

From profile MH110 set, the results of different rates of lift for different angles of attack can be analyzed. Table 1 shows the lift, drag and pressure for angles of attack from 0 to 10 degrees, with an increase of 1 degree.

Table 1: parameters according to the angle of attack

α [°]	C_l[-]	C_d [-]	C_l/C_d [-]
0.0	0.017	0.02460	0.6911
1.0	0.103	0.02491	4.1349
2.0	0.223	0.02422	9.2073
3.0	0.343	0.02328	14.7337
4.0	0.462	0.02500	18.4800
5.0	0.581	0.02667	21.7848
6.0	0.676	0.02644	25.5673
7.0	0.769	0.02677	28.7262
8.0	0.856	0.02876	29.7636
9.0	0.923	0.03577	25.8037
10.0	0.977	0.04411	22.1492

Table 1 shows that the highest value of Cl is to angle of attack 10° but the optimal lift-drag ratio is when α=8°. Whereas the blade is designed for a wind speed pre-determined, it can be calculated the speed and therefore the resulting velocity. With the resulting velocity known, it is possible to draw the blade pitch angle (which is fixed) such as to reach the desired angle of attack, because it can be found with the subtraction of the angle between the resulting velocity and the Vr plane of rotation and the pitch angle.

According to [17], there is a specific velocity represented in Eq. (2) by λ. This parameter, which is a dimensionless number, is given by the relationship between the speed at the tip of the blade v_u and the velocity v of the wind.

$$\lambda = \frac{v_u}{v} \tag{2}$$

The speed of rotation v_u can be defined by the product of the angular velocity ω of the blade and its radius R as shown in Eq. (3).

$$v_u = \omega R \tag{3}$$

d) Geometry of the longitudinal profile

For [2], a specific speed $\lambda = 6$ is suitable for three-bladed rotor. Whereas the wind speed is v=10m/s, the rotation speed is 60m/s for a 1 meter radius rotor. The rotor in this configuration will work approximately at *573RPM*.

$$c(r) = \frac{2\pi R}{n} \cdot \frac{8}{9} \cdot \frac{1}{c_L \lambda_D^2 \frac{r}{R}} \tag{4}$$

Where

c - blade chord
R - radius of rotor
n - number of blades
c_L - lift coefficient
λ_D - tip speed ratio of design blade geometry
r - local radius

Solving the Eq. (4) for eighteen sections of the blade, it is possible to have the measures of the chord at these points, as shown in Fig. 3.

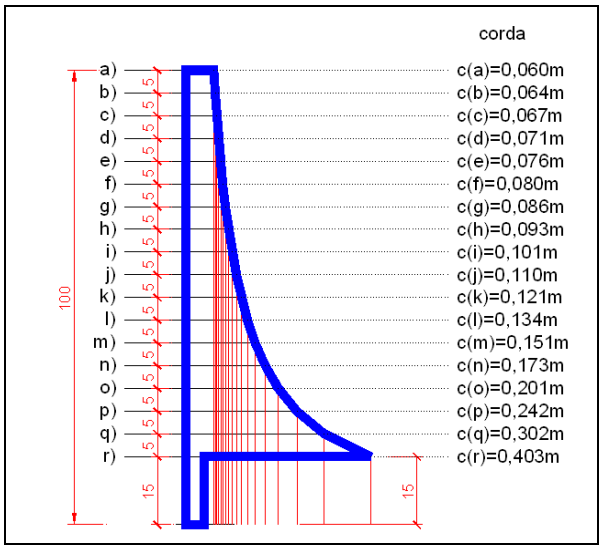

Figure 3: Dimensions of the blade chord for the defined sections

According to [18], the twist of the blade can be defined as in Eqs. (5) and (6)

$$\beta(r) = \gamma(r) + \alpha_A(r) \tag{5}$$

$$\gamma(r) = \arctan\left(\frac{3}{2}\frac{r}{R}\lambda_D\right) \tag{6}$$

where γ represents the angle between the relative velocity of the wind (geometric sum between wind and the speed of rotation of the blade) and the rotation speed of the blade. The α is the angle of attack.

The twist of the blade provides increased lift force that acts on the blade. However as it approaches the tip, the twist tends to reduce and the profile tends to have its cord parallel to the rotation speed, which is larger than the tip speed of the wind. Moreover, the part near to the root of the blade tends to have a chord and twist higher.

Figures 4 and 5 show the sections and their respective pitch angles along the blade. The blue circle in figure 4 represents the root, and the lower profile (magenta) represents the tip of the blade. The largest section, or profile, has chord 0.403m and pitch angle 28.521°, as shown in figure 4. This section is at 0.15m from the root of the blade. This drawing represents an ideal model.

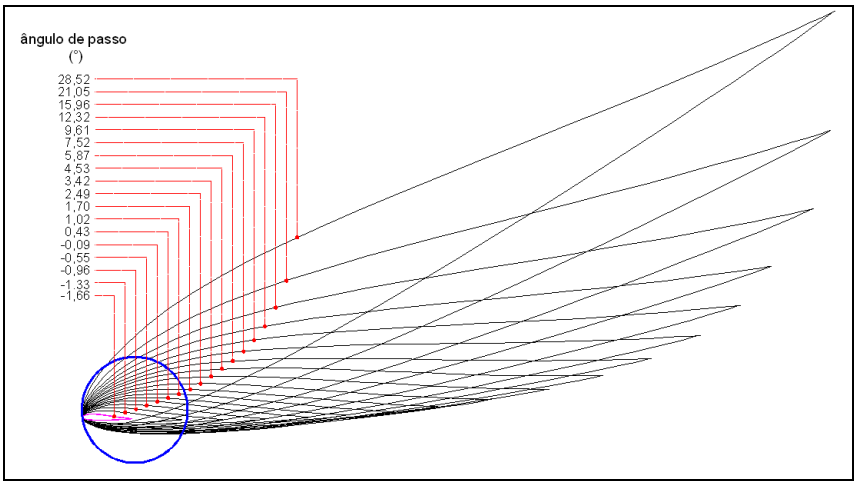

Figure 4: Pitch angle calculated for each section of the blade

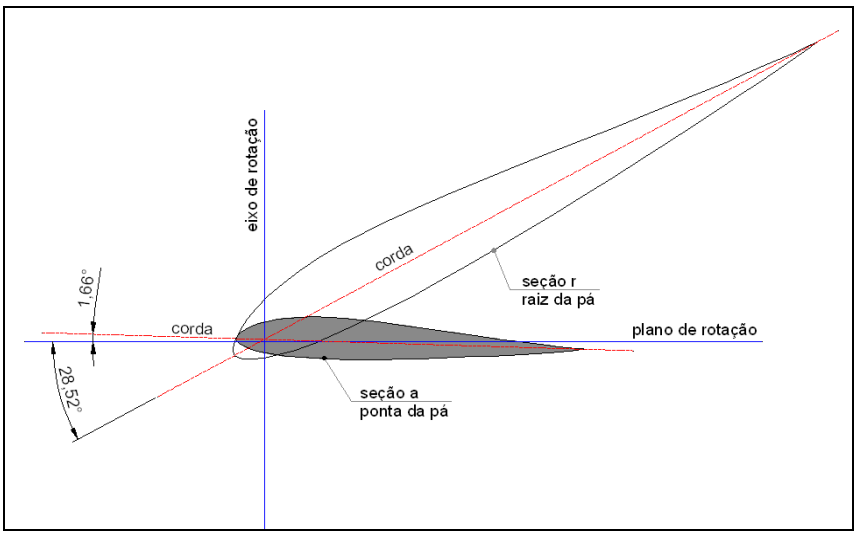

Figure 5: First and last pitch angle of the blade

The blade must be designed to operate without producing turbulence. Thus it is necessary a concordance between the shape from the calculations of chord and twist and surface that will be constructed. The flow along the blade surface should be laminar and have a minimum turbulence. To achieve this goal, it is necessary a smooth in the blade geometry. This process can provide aerodynamic losses as well the arising of high tension regions in the blade. The analysis by finite element method can assist to finding possible locations where high stresses can cause damage to the part.

Adopting this construction method of the blade geometry, it is possible to model the blade in three dimensions (Fig. 6) with the aid of the software Rhino3D from Robert McNeel & Associates.

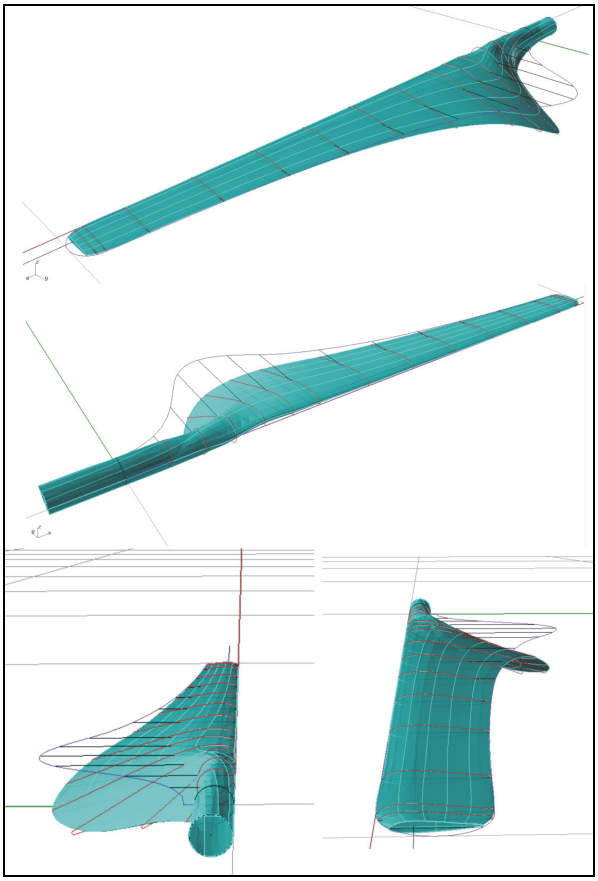

Figure 6: shape of the blade

3 MATERIAL PROPERTIES

To obtain mechanical properties used in this study composite specimens were moulded with epoxy and glass fiber unidirectional fabric maintaining the fibre volume fraction of 37%. The specimens were molded by Resin Transfer Molding (RTM) and compression processes. The compression process was used to obtain samples for the in-plane shear modulus through the tensile test of laminates ± 45° in accordance with ASTM D3518 [19] using eight laminate, since the used RTM system allows obtaining composites up to five laminates. The samples were cut and conducted to the ageing environment in hot water for 15 days / 50 ° C.

The properties were obtained for samples with and without ageing. Elastic moduli E_1 (fibre direction) and E_2 (transversal to the fibre direction), shear modulus G_{12}, Poisson's ratio ν_{12} and tensile strengths X_t (fibre direction) and Y_t (transversal to the fibre direction) were obtained from experimental tests.

Thus, to perform simulations, the software Abaqus/CAE 6.10 was used with properties obtained experimentally. However, as it was not possible in this study to obtain the compressive and in-plane shear strength properties, they were obtained using Micromechanics through the software Helius:CompositePro^{TM} Version 4.1

The material behaviour was considered to be elastic and the used properties for ageing and non-ageing cases were shown in tables 2 and 3.

Table 2: Material data obtained by experimental analysis

	NON-AGEING	AGEING
E_1	20,119 GPa	18,773 GPa
E_2	7,678 GPa	6,881 GPa
ν_{12}	0,234	0,217
$G_{12}G_{13}$, G_{23}	5,501 GPa	4,947 GPa

Table 3: Strength data obtained by experimental analysis and through Micromechanics

	NON-AGEING (MPa)	AGEING (MPa)
X_t	354,512	314,943
X_c	531,075	471,798
Y_t	82,129	86,813
Y_c	99,346	105,012
$S_A = S_T$	121,830	121,830

4 STRUCTURAL ANALYSIS

Considering the small size of the rotor (*Ø~2.00m*), the structural aspects reported in this research are

- Mechanical strength of the blade due to
  - constant wind load (average)
  - cross load wind
  - load of greater turbulence in the wind
  - centrifugal force
  - self-weight
  - gyroscopic force

4.1 Mechanical strength

Loads acting on the blade due to the interaction with the air flow are uniform aerodynamic forces. Assuming that apparent speed v_w (resulting velocity) is constant, there is a distribution of forces on the blade when it is operating. This distribution occurs in two ways: thrust (Eq. 7) and rotational force (Eq. 8), were ρ represents the air density considered 1.29 kg/m³ at sea level, c represents the chord and is function of length of the blade and dr is the component that represents the infinitesimal thickness ring considered for calculating the swept area of the blade, where there will be the interaction of rotational speed and the wind

$$dT = \frac{\frac{1}{n}\left(\frac{8}{9}\frac{\rho}{2}v_w^2\right)2\pi r dr}{c} \tag{7}$$

$$dU = \frac{\frac{2\pi R}{n\lambda_D}\left(\frac{16}{27}\frac{\rho}{2}v_w^2\right)dr}{c} \tag{8}$$

There is also forces due to the gusts, causing variation in dT and high instantaneous pressure in the blade, however if the thrust is calculated with the resulting velocity considering wind speed and rotational speed high, it can be considered that the thrust is calculated to have gusts of wind.

Forces due to yaw, gyroscopic and coriolis were disregarded because this movement is usually slow in relation to rotation of the blades. The inertia due to the braking system was also disregarded because the rotor has no mechanical brake.

According to [17], for large turbines, the blade weight influences a cyclic loading. For rotors with $Ø = 20m$, the influence is small, for rotors with $Ø < 5m$, this load is irrelevant.

Aerodynamic loads were calculated for speed of 40m/s. Simulation were performed for 6, 8 and 10 layer with thicknesses of 0.0006m each one.

Figure 7 shows the blade modelled by a mesh of 4154 triangular elements with 2079 nodes and shows the results of displacements for a lamination sequence of ten layers with fibre orientation of 0°. Each layer has 0.0006m thickness and the wind speed is 40m/s (wind speed above the average recorded in Brazil and used in simulations to verify the occurrence of failure). The largest displacement (0.128m) is observed at the tip of the blade with 8 layers.

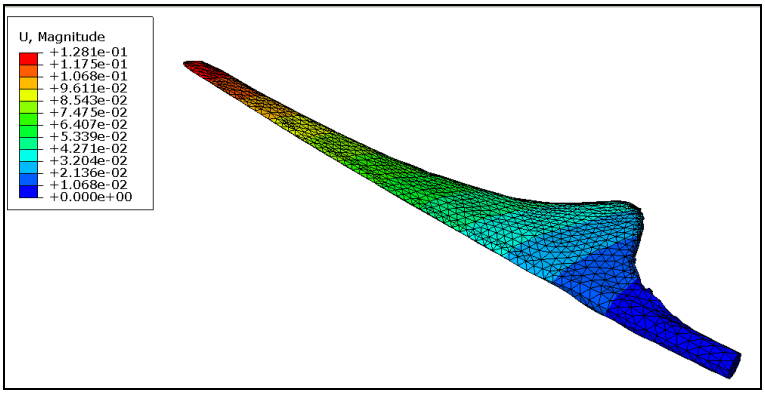

Figure 7: Displacement of the blade (non-ageing – 8 layers)

Displacement values for the other lamination types studied and for ageing situations are given in Tables 4, 5 and 6.

Figure 8 shows the stress distribution on the blade also for ten layer of 0.0006m thickness without ageing and shows that the most stressed area is close to the root, i.e., near to the shaft.

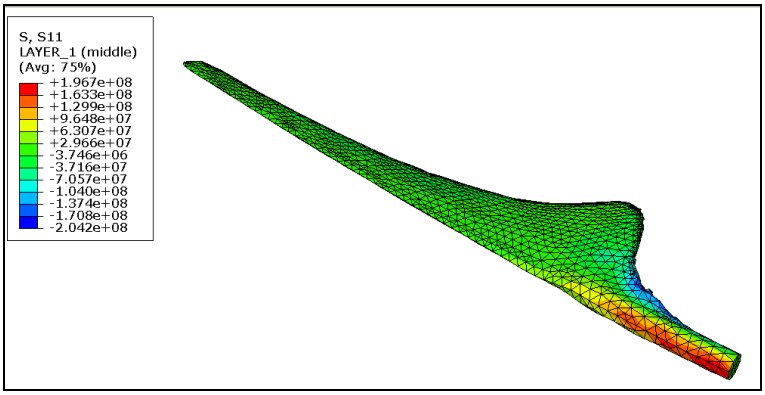

Figure 8: Stress σ_{11} (longitudinal axis direction of the blade - non-ageing- 8 layers)

Objects made of fibreglass will typically have different layers in order to obtain some properties according to its use. Composite materials consisting of fibre and matrix are subjects to failure due to delamination, loss of adhesion between fibre and matrix, matrix rupture or rupture of the fibre.

There are some criteria that mathematically describe the conditions under which a composite material may fail. Among the most common criteria is the Hashin criterion [20], which considers failure modes in fibres and matrix in compression and tension, given by the following equations.

Fibre tension mode

$$\left(\frac{\sigma_{11}}{X_t}\right)^2+\left(\frac{\sigma_{12}{}^2+\sigma_{13}{}^2}{S_A{}^2}\right)=1 \tag{9}$$

Fibre compression mode

$$\left(\frac{\sigma_{11}}{X_c}\right)^2=1 \tag{10}$$

Matrix tension mode

$$\frac{1}{Y_t}(\sigma_{22}+\sigma_{33})^2+\frac{1}{S_T{}^2}\left(\sigma_{23}{}^2-\sigma_{22}\sigma_{33}\right)+\frac{1}{S_A{}^2}\left(\sigma_{12}{}^2+\sigma_{13}{}^2\right)=1 \tag{11}$$

Matrix compression mode

$$\frac{1}{Y_c}\left(\frac{Y_c{}^2}{4S_T{}^2}-1\right)(\sigma_{22}+\sigma_{33})+\frac{1}{4S_T{}^2}\left(\sigma_{22}{}^2-\sigma_{33}{}^2\right)+\frac{1}{S_T{}^2}\left(\sigma_{23}{}^2-\sigma_{22}\sigma_{33}\right)+\frac{1}{S_A{}^2}\left(\sigma_{12}{}^2+\sigma_{13}{}^2\right)=1 \tag{12}$$

The strength properties of the material in non-ageing and ageing situations are given in table 3.

Taking into account the Hashin failure criterion, simulations were performed with different number of layers. Table 4 shows that according to Hashin failure criterion, fail occurs in the matrix tension and fibre tension.

Table 4: Results of computational analysis for 6 layers

Material	Thickness each layer (m)	Displacement (m)	layer	Hashin failure criterion			
				Fibre Compression	Fibre Tension	Matrix Compression	Matrix Tension
Non-ageing	0,0006	0,223	1	0,6519	0,9172	0,2396	4,580
			2	0,3919	0,9288	0,2162	2,272
			3	0,3866	0,9405	0,1931	0,8146
			4	0,4211	1,029	0,5620	1,609
			5	0,4570	1,138	0,7528	2,808
			6	0,5374	1,253	0,4625	4,410
Ageing 15 days	0,0006	0,227	1	0,8096	1,043	0,1892	4,044
			2	0,4837	1,058	0,2006	2,018
			3	0,4437	1,073	0,1492	0,7426
			4	0,4828	1,172	0,4834	1,420
			5	0,5235	1,295	0,6938	2,425
			6	0,7201	1,423	0,4786	3,756

An iterative process of analysis, involving variables such as number of layers may be implemented to reach the most suitable design by reducing material for the blade. Tables 5 and 6 present results of displacements and Hashin failure criterion for laminates with 8 and 10 layers, respectively.

Table 5: Results of computational analysis for 8 layers

Material	Thickness each layer (m)	Displacement (m)	layer	Hashin failure criterion			
				Fibre Compression	Fibre Tension	Matrix Compression	Matrix Tension
Non-ageing	0,0006	0,124	1	0,2324	0,5953	0,1907	0,9826
			2	0,2241	0,6052	0,1773	0,7188
			3	0,2438	0,6179	0,1641	0,3985
			4	0,2644	0,6336	0,1526	0,2719
			5	0,2858	0,6946	0,2682	0,4756
			6	0,3084	0,7666	0,1938	0,8087
			7	0,3336	0,8421	0,4387	1,271
			8	0,3598	0,9211	0,3243	1,863
Ageing 15 days	0,0006	0,128	1	0,2978	0,7579	0,1769	0,9395
			2	0,2840	0,7714	0,1641	0,6790
			3	0,3085	0,7873	0,1791	0,3792
			4	0,3340	0,8077	0,1480	0,2753
			5	0,3630	0,8869	0,2738	0,4743
			6	0,3935	0,9781	0,2056	0,7941
			7	0,4252	1.074	0,4634	1,235
			8	0,4582	1,174	0,3478	1,796

Table 6 shows that for ten layers each one with thickness of 0.0006m and wind speed of 40m/s, the blade will displace about 0,06m and no failure will occur.

Table 6: Results of computational analysis for 10 layers

Material	Thickness each layer (m)	Displacement (m)	layer	Hashin failure criterion			
				Fibre Compression	Fibre Tension	Matrix Compression	Matrix Tension
Non-ageing	0,0006	0,060	1	0,1425	0,3501	0,1193	0,4649
			2	0,1369	0,3593	0,1121	0,3239
			3	0,1436	0,3691	0,1049	0,2123
			4	0,1555	0,3809	0,0978	0,1460
			5	0,1678	0,3945	0,0907	0,1495
			6	0,1806	0,4314	0,1460	0,1836
			7	0,1939	0,4733	0,1094	0,2968
			8	0,2085	0,5172	0,1212	0,4149
			9	0,2248	0,5630	0,2291	0,5887
			10	0,2418	0,6107	0,1957	0,8011
Ageing 15 days	0,0006	0,065	1	0,1835	0,4439	0,1124	0,4187
			2	0,1761	0,4567	0,1055	0,2918
			3	0,1828	0,4696	0,0987	0,1918
			4	0,1978	0,4845	0,0919	0,1285
			5	0,2133	0,5020	0,0861	0,1310
			6	0,2295	0,5497	0,1440	0,1794
			7	0,2462	0,6027	0,1103	0,2921
			8	0,2658	0,6582	0,1243	0,3975
			9	0,2865	0,7162	0,2342	0,5587
			10	0,3079	0,7766	0,2032	0,7669

For the simulations conducted, the composite material with 10 layers is the adequate and safety for the blade.

5 CONCLUSIONS

The article presented succinctly the modeling and computer simulation of the structure of a blade, made in fiberglass, for a small wind turbine, with 2.00m diameter. The 3D modeling took into account aerodynamic aspects to enhance the conversion of kinetic energy of wind into electrical energy. Loads due to wind action on the blades were considered.

Generally the mechanical properties tested showed a decrease if compared situations with and without material ageing, however Y_t and Y_c showed an increase that may be related with a second crosslinking of the polymeric matrix chains.

From simulation by finite element method the thickness of the blade was proposed. According to results presented in tables 4, 5 and 6, it is evident that the smaller blade thickness, the greater displacement at the tip (with encastre in the root of the blade) with the applied load.

Results also show that, when it was considered Hashin failure criterion for the studied material it was noted that the failure modes in the matrix tend to be the dominant failure modes, but also failure occur in the fibre direction, mainly on ageing material.

The simulations took into account the displacement, mainly at the blade tip, which occurs after the loads applying. This displacement should be small to avoid the collision of the blade with the tower or wind turbine support stem.

For a better accuracy in the simulations, a study of wind data from the site where the turbine will be installed should be made. Data from this study can assist developing design of blades for

small wind turbines. Virtual simulations of structures, as well as simulations of airfoils made by computer, have become very important tools when trying to design aerodynamic equipment.

The ageing study aids in predicting the useful life of the materials. By knowing the degradation process and changes occurred in the properties of composite materials after a set time of use, it is possible to optimize designs in order to reduce costs and increase the safety and durability of the equipment. In future works other accelerated ageing situations will be studied.

6 ACKNOWLEDGEMENTS

The financial support of CNPq, CAPES, FAPERGS and PROPESQ/UFRGS is gratefully acknowledged.

REFERENCES

[1] Tolmasquin M. T., (2003), Fontes renováveis de energia no Brasil. Interciencia, Rio de Janeiro.

[2] Burton T. Sharpe D. Jenkins N. Bossanyi E., (2001), Wind energy: handbook. Ed. John Wiley & sons, England.

[3] Epaarachchi J. Clausen P., (2006), The development of a fatigue loading spectrum for small wind turbine blade. Journal of Wind Engineering and Industrial Aerodynamics, p. 207-223.

[4] Shokrieh M. Rafiee R. (2006), Simulation of fatigue failure in a full composite wind turbine blade. Composite Structures, p. 332-342.

[5] Neto F. Pardini L., (2006), Compósitos estruturais: ciência e tecnologia. Ed. Edgard Blücher, Brasil.

[6] Piva A.M. Wiebeck H., (2004), Reciclagem do Plástico**-**Como fazer da reciclagem um negócio lucrativo. Ed. Artliber, Brasil.

[7] Khan L.A. Nesbitt A. Day R.J. (2010) Hygrothermal degradation of 977-2A carbon/epoxy composite laminates cured in autoclave and Quickstep. Composites: Part A, 41, 942-953.

[8] Nakai S. Ikegaki H. Hamada N. Takeda. (2000) Degradation of braided composites in hot water. Composites Science and Technology 60 325±331.

[9] Dionysis E. Mouzakis B. Helen Zoga A. Costas Galiotis A.B. (2008), Accelerated environmental ageing study of polyester/glass fiber reinforced composites (GFRPCs). Composites: Part B 39 467–475.

[10] Yunying W. Jiangyan M. Qing Z. Shuhua Q. (2010), Accelerated Ageing Tests for Evaluations of a Durability Performance of Glass-fiber Reinforcement Polyester Composites. J. Mater. Sci. Technol., 26(6), 572-576.

[11] Mannberg P. Giannadakis K. Jakovics A. Varna J. (2010), Moisture Absorption and Degradation of Glass Fiber/Vinylester Composites. Modelling for Material Processing 157-162.

[12] Faguaga E. Pérez C.J. Villarreal N. Rodriguez E.S. Alvarez V. (2012), Effect of water absorption on the dynamic mechanical properties of composites used for windmill blades. Materials and Design 36 609–616.

[13] Vauthier E. Abry J. C. Bailliezb T. Chateauminois A. (1998), Interactions Between Hygrothermal Ageing and Fatigue Damage in Unidirectional Glass/Epoxy Composites. Composites Science and Technology 58 6877692.

[14] Chateaurninois A.Vincent L. (1994), Study of the interfacial degradation of a glass-epoxy composite during hygrothermal ageing using water diffusion measurements and dynamic mechanical thermal analysis. POLYMER Volume 35 Number 22.

[15] Jureczko M. et al, (2005), Optimization of Wind Turbine Blade. Journal of Materials Processing Technology, p. 463-471.

[16] Hepperle M. (2004), Other Airfoils – MH110, free profile. www.mh-aerotools.de.

[17] Carvalho P. (2003), Geração Eólica. Ed. Imprensa Universitária, Fortaleza, Brasil.

[18] Gasch R. Twele J. (2002), Wind Power Plants, Solarpraxis AG, Germania.

[19] American Society for Testing and Materials (2007), ASTM D3518 Standard Test Method for In-Plane Shear Response of Polymer Matrix Composite Materials by Tensile Test of a ±45° Laminate, ASTM International.

[20] Hashin Z. (1980), Failure criteria for unidirectional fiber composites, J. of Applied Mechanics,47, 329-334.